FORCE-INTERVAL RELATIONSHIP IN HEART MUSCLE OF MAMMALS

A Calcium Compartment Model

VINCENT J. A. SCHOUTEN, JURJEN K. VAN DEEN, PETER DE TOMBE, AND ALETTUS A. VERVEEN
Departments of Cardiology and Physiology, State University of Leiden, Wassenaarseweg 62, 2333 AL Leiden, The Netherlands

ABSTRACT A mathematical model was derived that describes peak force of contraction as a function of stimulus interval and stimulus number in terms of Ca^{2+} transport between three hypothetical Ca^{2+} compartments. It includes the conventional uptake and release compartments and recirculation of a fraction r of the activator Ca^{2+}. Peak force is assumed to be proportional to the amount of activator Ca^{2+} released from the release compartment into the sarcoplasm. A new extension is a slow exchange of Ca^{2+} with the extracellular space via an exchange compartment. Six independent parameters were necessary to reproduce the different effects of postextrasystolic potentiation, frequency potentiation, and post-rest potentiation in isolated heart muscle from the rat. The normalized steady state peak force (F/F_{max}) under standard conditions varied by a factor of ten between preparations from rat heart. Analysis with the model indicated that most of this variation was caused by two variables: the Ca^{2+} influx per excitation and the recirculating fraction of activator Ca^{2+}. The influence of the Ca^{2+} antagonist nifedipine of the force-interval relationship was reproduced by the model. It is concluded that the model may serve to analyze the variability of contractile force and the mode of actions of drugs in heart muscle.

INTRODUCTION

It is generally accepted that the rise of intracellular free Ca^{2+} concentration after an electrical stimulus determines the tension development of heart muscle (Fozzard, 1977; Wohlfart and Noble, 1982; Fabiato, 1983). Several models of cellular Ca^{2+} transport have been developed to describe the force-interval relationship in mammalian muscle. The general hypothesis is that the action potential triggers Ca^{2+} release from an intracellular compartment into the sarcoplasm. This activator Ca^{2+} induces force production by the contractile filaments. An uptake compartment sequesters a fraction of the activator Ca^{2+} and the Ca^{2+} that enters the cell during the action potential. Transport of Ca^{2+} from the uptake to the release compartment is assumed to occur with a time constant of ~1 s (Manring and Hollander, 1971; Kaufmann et al., 1974; Morad and Goldman, 1973; Edman and Johannsson, 1976; Wohlfart, 1979). The delayed replenishment of the release compartment via the uptake compartment has been postulated to explain the fact that a change of the duration of one action potential has an inotropic effect predominantly on the next contraction and not on the concomitant contraction (Antoni et al., 1969; Braveny and Sumbera, 1970).

The previous models account for many aspects of the force-interval relationship, however, not for the complex mechanical restitution curve of rat myocardium (Fig. 1 *A*). A third exchange compartment has been postulated (Fig. 1 *B*) to account for the relatively strong contractions at stimulus intervals of ~100 s. The physiological or anatomical counterparts for the three compartments may be the sarcoplasmic reticulum for the uptake and release compartments (Katz, 1976) and a combination of the Na^+/Ca^{2+}-exchange mechanism and the Na^+/K^+ pump for the exchange compartment (Schouten, manuscript submitted for publication). Presently a mathematical description is given of the three-compartment model to obtain quantitative statements about the consequences of such a model.

DEFINITION OF THE "MINIMUM MODEL"

In the literature two different approaches to design a model of excitation-contraction coupling of Ca^{2+} transport in heart muscle can be distinguished: the abstract approach and the fundamental approach (models of data and models of systems, respectively. See DiStefano and Landaw, 1984).

Models of Data

Blinks and Koch-Weser (1961) described the force-interval relationship in abstract terms of a positive and a negative inotropic effect of activation (PIEA and NIEA). The "effects" were assumed to be cumulative and to decay with different time constants. Furthermore, they postu-

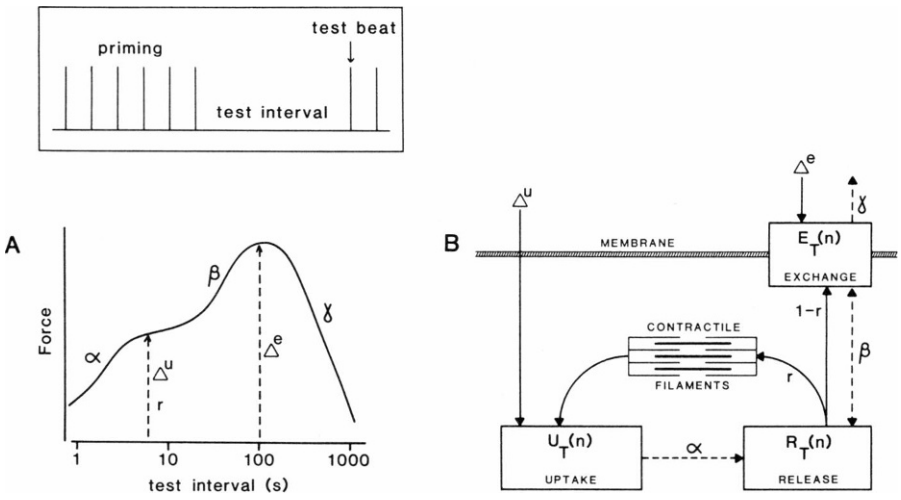

FIGURE 1 A model of Ca^{2+} transport in heart muscle fibers. The model was based on the analysis of the mechanical restitution curves of trabeculae from rat heart. The curve represents peak force of the test contraction elicited after a single variable test interval, interpolated in a train on constant intervals (*inset*). An example is shown in *A*. The parameters of the model (*B*) determine specific parts of the restitution curve, as indicated in *A*. Dashed lines in *B* represent slow Ca^{2+} transport with rate constants α, β, and γ. Δ^e and Δ^u represent the amounts of Ca^{2+} transported from the extracellular space into the intracellular compartments with each excitation. Solid lines represent instantaneous Ca^{2+} transport. See the text for a further explanation.

lated an independent "rested state contraction," i.e., their model consisted of five independent parameters that were related to specific responses of heart muscle to various stimulation patterns. The properties of heart muscle vary greatly with the species of animal and region of the heart from which the preparation is taken. Much of this variation could, however, be explained on the basis of the three parameters PIEA, NIEA, and the rested state contraction (Koch-Weser and Blinks, 1963).

During the past twenty years the crucial role of Ca^{2+} in the regulation of contraction has been established, and the complex force-interval relationship is currently described in terms of accumulation of Ca^{2+} in, and time-dependent transport between, intracellular compartments. In the models of data neither the nature of the compartments nor the transport processes is crucial. A model compartment may represent a restricted volume within the cell or a specific group of binding sites distributed throughout the cell. Transport may represent displacement of Ca^{2+} or the transition between different states. Thus it is the effect (an aspect of the force-interval relationship) rather than the underlying physiological mechanism that appears in the model. It follows that each parameter in the model should represent a specific effect observed in the experimental preparation. If possible, it should be evidenced that the effects are independent or, in other words, it should be excluded that a certain effect is a mere coincidence of two or more others.

Thus, the best model has the minimum number of parameters required for an adequate fit of the data (Garfinkel and Fegley, 1984), and this is our definition of the minimum model. In previous models the independence of the parameters generally could not be verified (Manring and Hollander, 1971 [7 parameters]); and often the number of model parameters exceeded the number of experimentally identified effects (e.g., Posner and Berman, 1967 [9 parameters]; Wohlfart, 1982 [16 parameters]), or the authors did not give any justification for the parameters (e.g., Markhasin and Mil'shtein, 1979 [more than 6 parameters?]; Tsaturyan and Izakov, 1979 [11 parameters]). In our opinion such models are likely to contain superfluous features.

Models of Systems

The alternative approach is to gather data from the literature concerning fundamental mechanisms relevant to the regulation of contraction (kinetics of the interaction of Ca^{2+} at the contractile filaments, the Ca^{2+}–Mg^{2+} ATPase at the sarcoplasmic reticulum, etc.). The combination of a number of such mechanisms may result in a system model which reproduces all kinds of phenomena and eventually also the force-interval relationship. In its most extreme form the system model includes all aspects of heart muscle physiology and becomes the maximum model. A modest attempt has been reported by Kaufmann et al. (1974). Their model (~20 parameters) included simplified formalizations of the kinetics of Ca^{2+} transport by the sarcoplasmic reticulum, the mitochondria, and the sarcolemma. Of course, it is difficult to establish the relative importance of each of the many parameters to the force-interval relationship.

This problem may be illustrated as follows: The model developed by Kaufmann et al. (1974) was extended by Wong (1981) with more detailed kinetics of the inward transport of Ca^{2+} during the action potential and of the interaction of Ca^{2+} with the contractile filaments. The

final model contained 30 parameters. A few years later Adler et al. (1985) extended the model further with a Ca^{2+} buffer in the sarcoplasmic reticulum, but made such rigorous simplifications that the total number of parameters was reduced to 11. As a result, the accuracy of the simulated force-interval relationship was improved then.

There were two main reasons to develop a new version of the model of the force-interval relationship: (*a*) the literature does not provide a real minimum model; and (*b*) the available models do not reproduce the type of mechanical restitution observed in heart muscle of the rat (see Introduction).

THE MODEL

The model depicted in Fig. 1 *B* is similar to the conventional model with respect to the presence of an uptake and release compartment, the inflow of an amount Δ^u per action potential into the uptake compartment, and the recirculation of a fraction r of activator Ca^{2+} (cf. Morad and Goldman, 1973; Wohlfart, 1979). Furthermore a slow transport of Ca^{2+} from the release compartment to the extracellular space has been generally assumed to account for the weak rested state contraction. New in the present model is the introduction of an exchange compartment, which controls such slow transport in both directions. Filling of this compartment occurs through the excitation dependent influx Δ^e.

A minimum number of six parameters was necessary in the model to meet the variation in the mechanical restitution curve (Fig. 1 *A*) following different stimulation patterns. Three rate constants of Ca^{2+} transport, α, β, and γ, account for the three phases of mechanical restitution. The inflow of the quantities Δ^u and Δ^e allow for the independent variation of the amplitude of the early and late phases of the mechanical restitution curve. The recirculating fraction r represents the excitation-dependent coupling between the early and late phase as observed during post-rest potentiation, and r also accounts for the exponential decay of postextrasystolic potentiation.

To obtain a simple model the following assumptions are proposed: (*a*) Force of contraction is proportional to the amount of Ca^{2+} released upon excitation from the release compartment. This means that the kinetics of Ca^{2+} binding to the contractile filaments, and the influence of sarcomere length are not considered in any detail. (*b*) The release compartment empties completely with each excitation. (*c*) The events of excitation, Ca^{2+} release, contraction and Ca^{2+} uptake by the uptake compartment occur within an infinitesimal time. The only time-dependent processes are the Ca^{2+} transport from the uptake to the release compartment, between the release and the exchange compartments in both directions and from the exchange compartment to the extracellular space. As a consequence, the model will not apply accurately to the events that occur after very short intervals, when the duration of the processes of Ca^{2+} release and contraction cannot be neglected. A detailed description of the time course of the events during the contractions has been given by Wallinga-de Jong et al. (1981) and by Landau and Valentini (1982). (*d*) Finally, it is assumed that the transport of Ca^{2+} between the release and exchange compartments does not influence the content of the latter. This implies that the exchange compartment is assumed to be much larger than the release compartment.

Ca^{2+} Content of the Compartments As a Function of Time

The unidirectional Ca^{2+} transport from the uptake to the release compartment is assumed to be proportional to the amount of Ca^{2+} in the uptake compartment, $U(t)$, according to the differential equation

$$\frac{d\,U(t)}{dt} = -\alpha \cdot U(t), \tag{1}$$

where α is a constant and t is the time. Given the boundary conditions $U(0) = U_0$ and $U(\infty) = 0$ it follows that

$$U(t) = U_0 \cdot e^{-\alpha t}. \tag{2}$$

From the exchange compartment Ca^{2+} is transported to the extracellular space and to the release compartment. For simplicity the latter transport is assumed to have no effect on the Ca^{2+} content of the exchange compartment, as if the volume of this compartment is much larger than the volume of the release compartment. Furthermore, the transport to the extracellular space is assumed to be proportional to the amount of Ca^{2+}, $E(t)$ in the exchange compartment, hence the differential equation and its solution (boundary conditions $E(0) = E_0$ and $E(\infty) = 0$) are

$$\frac{dE(t)}{dt} = -\gamma \cdot E(t) \tag{3}$$

$$E(t) = E_0 \cdot e^{-\gamma t}, \tag{4}$$

where γ is constant. The Ca^{2+} transport between the exchange and release compartments in both directions is assumed to obey diffusion kinetics, i.e., the flow of mass is proportional to the concentration difference, as represented by the differential equation

$$\frac{dm}{dt} = \delta \cdot \left(\frac{E(t)}{V_E} - \frac{R(t)}{V_R} \right), \tag{5}$$

where m is the net transported mass in the direction of the release compartment, $E(t)$ and $R(t)$ are the amounts of Ca^{2+} in the exchange and release compartments, V_E and V_R are the volumes of the compartments and δ is a constant. For further analysis it is convenient to introduce the following substitutions

$$E'(t) = \frac{V_R}{V_E} \cdot E(t) \tag{6}$$

$$\beta = \frac{\delta}{V_R}. \tag{7}$$

Thus Eq. 5 becomes

$$\frac{dm}{dt} = \beta \cdot \{E'(t) - R(t)\}. \quad (8)$$

The release compartment gains Ca^{2+} from the uptake (Eq. 1) and from the exchange compartment (Eq. 8)

$$\frac{dR(t)}{dt} = \alpha \cdot U(t) + \beta \cdot \{E'(t) - R(t)\}. \quad (9)$$

Using Eqs. 2, 4, and 6, the solution for $R(t)$ can be found, given the boundary conditions $R(0) = 0$ (all Ca^{2+} released at $t = 0$) and $R(\infty) = 0$

$$R(t) = U_0 \cdot \frac{\alpha}{\beta - \alpha} \cdot (e^{-\alpha t} - e^{-\beta t}) + E'_0 \cdot \frac{\beta}{\gamma - \beta} \cdot (e^{-\beta t} - e^{-\gamma t}). \quad (10)$$

To simplify the notation we introduce the functions f and g

$$f = \frac{\alpha}{\beta - \alpha} \cdot (e^{-\alpha t} - e^{-\beta t}) \quad \text{and} \quad g = \frac{\beta}{\gamma - \beta} \cdot (e^{-\beta t} - e^{-\gamma t}). \quad (11)$$

Eq. 10 gives the amount of Ca^{2+} available for release when an interval t has elapsed since the previous release. Under the assumption that peak force of contraction is proportional to the amount of released Ca^{2+} this equation describes mechanical restitution (Fig. 1 *A*).

Beat-to-Beat Changes

In this section equations will be derived for the Ca^{2+} content of the compartments as a function of the number of stimulus intervals of constant duration. At the end of each stimulus interval the amount of Ca^{2+} in the three compartments is given by Eqs. 2, 4, and 10. These serve as the starting condition for the next cycle and recurrence relations are obtained, except for the release compartment from which all Ca^{2+} is released, i.e., at the beginning of each stimulus interval the release compartment is empty. In Fig. 2 the sequence of events during the excitation-contraction cycle is indicated, and the variables are defined.

We define $E_{o,T}(n)$ as the amount of Ca^{2+} in the exchange compartment at the beginning of the nth interval of T seconds. During every excitation a constant amount, Δ^E, of Ca^{2+} flows into the exchange compartment. According to the basic assumptions the transport between the release and exchange compartments does not influence the content of the latter ($V_R << V_E$). By substitution of $\Delta^e = \Delta^E \cdot V_R/V_E$, and with Eqs. 4 and 6 it follows that

$$E'_{o,T}(n+1) = E'_{o,T}(n) \cdot e^{-\gamma T} + \Delta^e. \quad (12)$$

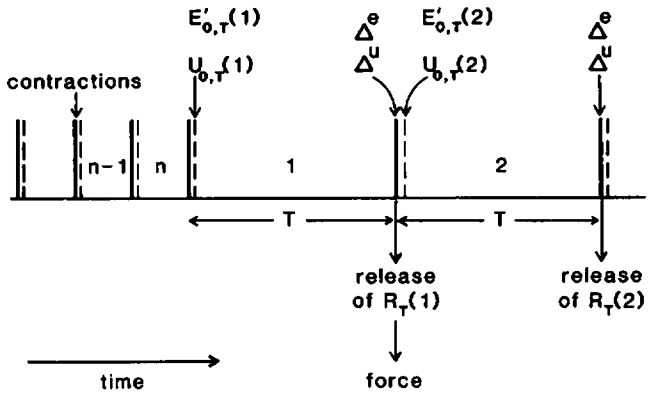

FIGURE 2 The parameters and variables of the model as defined during the excitation cycles. From the left to the right the scheme shows the last four of a train on n contractions. Then the interval between the contractions changes to T s, and the first interval is labeled 1. $E'_{o,T}(1)$ and $U_{o,T}(1)$ are the contents of the exchange and uptake compartments, respectively, at the beginning of interval 1. At T s the stimulus induces a complete release of the content $R_T(1)$ of the release compartment, the fraction r of $R_T(1)$ and the amount Δ^u flow into the uptake compartment, and the amount Δ^e flows into the exchange compartment. Within an infinitely short time the starting conditions, $E_{o,T}(2)$ and $U_{o,T}(2)$ for the second cycle are settled.

In the steady state ($n \longrightarrow \infty$), $E'_{o,T}(n)$ becomes constant

$$E'_{o,T}(\infty) = \frac{\Delta^e}{1 - e^{-\gamma T}}. \quad (13)$$

The solution for Eq. 12 is

$$E'_{o,T}(n) = \{E'_{o,T}(1) - E'_{o,T}(\infty)\} \cdot e^{-\gamma T(n-1)} + E'_{o,T}(\infty). \quad (14)$$

The uptake compartment derives Ca^{2+} from three sources: (*a*) Let the nth cycle start with $U_{o,T}(n)$. According to Eq. 2 this is reduced to $U_{o,T}(n) \cdot e^{-\alpha T}$ at the end of the interval, and this amount contributes to the next cycle. (*b*) A fraction, r, of the released Ca^{2+} (Eq. 10) is taken up by the uptake compartment. (*c*) During each excitation an amount Δ^u of Ca^{2+} flows from the extracellular space into the uptake compartment. $U_{o,T}(n+1)$ then equals the sum of the above three contributions.

$$U_{o,T}(n+1) = U_{o,T}(n) \cdot e^{-\alpha T} + r \cdot \{f \cdot U_{o,T}(n) + g \cdot E'_{o,T}(n)\} + \Delta^u. \quad (15)$$

In the steady state ($n \longrightarrow \infty$), $U_{o,T}(n)$ is constant, hence

$$U_{o,T}(\infty) = \frac{r \cdot g \cdot E'_{o,T}(\infty) + \Delta^u}{1 - e^{-\alpha T} - r \cdot f}. \quad (16)$$

The solution of the recurrence relation of Eq. 15 is

$$U_{o,T}(n) = \left\{\frac{r \cdot g \cdot (E'_{o,T}(0) - E'_{o,T}(\infty))}{e^{-\gamma T} - e^{-\alpha T} - r \cdot f}\right\} \cdot e^{-\gamma T(n-1)} + \left\{U_{o,T}(0) - U_{o,T}(\infty) - \frac{r \cdot g \cdot (E'_{o,T}(0) - E'_{o,T}(\infty))}{e^{-\gamma T} - e^{-\alpha T} - r \cdot f}\right\} \cdot (e^{-\alpha T} + r \cdot f)^{n-1} + U_{o,T}(\infty). \quad (17)$$

The content, $R_T(n)$, of the release compartment at the end of the nth interval of T seconds follows from Eqs. 10 and 11 by substitution of $R_T(n)$ for $R(t)$, $U_{o,T}(n)$ for U_o and $E'_{o,T}(n)$ for E'_o

$$R_T(n) = f \cdot U_{o,T}(n) + g \cdot E'_{o,T}(n). \quad (18)$$

This expression describes peak force as a function of stimulus number at constant intervals of duration T. Model simulations can be preformed for any stimulus protocol, if at every change of T the number n is reset to one.

MODEL SIMULATIONS

Mechanical Restitution

A large quantitative variation in the mechanical responses has been observed between the individual trabeculae isolated from rat heart. With respect to the qualitative effects of various stimulus patterns on the different phases of mechanical restitution all preparations behaved similarly (Schouten et al., manuscript submitted for publication). One set of parameter values was estimated that resulted in representative simulations of the muscle responses to the different stimulus patterns. In Table I the parameter values are given that were used for all simulated responses in this paper. The recirculating fraction is a dimensionless constant. The rate constants α, β, and γ are in per seconds. Twitch amplitude of the trabeculae was found to be maximal (F_{max}) at a calcium concentration of 2.5 mM, given a temperature of 26°C and nearly optimal muscle length (Schouten et al., manuscript submitted for publication). The experimentally measured peak force (F) was normalized to F_{max}, resulting in the dimensionless fraction F/F_{max}. In the model, peak force is assumed to be proportional to the released amount of Ca^{2+}, $R_T(n)$. To scale the model the values of the parameters Δ^u and Δ^e were chosen such that in the model simulations $R_T(n) = 1$ corresponds to $F = F_{max}$ in the heart muscle preparations. It follows that Δ^u and Δ^e can be regarded as dimensionless fractions. In the next three paragraphs the simulations of mechanical restitution are presented. The sensitivity of the results to variation of the parameters is shown in the graphs.

Variation of Priming Frequency. The stimulation protocol is depicted in Fig. 3 *A* (*inset*). An increase of the priming frequency causes an increase of force at all test intervals (Fig. 3 *A*). Since the content of the exchange compartment in the model is very sensitive to the frequency of stimulation this protocol is particularly suitable to determine the magnitude of Δ^e. The influence of Δ^e on the mechanical restitution curve is shown in Fig. 3 *B*.

Extrasystoles. The strength of contractions in heart muscle increases drastically after a few very short stimulus intervals (extrasystoles). In the model such post-extrasystolic potentiation is due to Ca^{2+} accumulation in the uptake compartment. The effect of extrasystoles is an increase of peak force predominantly at test intervals of ~10 s, and the increase of peak force is approximately equal to the product of the number of extrasystoles and Δ^u (Fig. 3 *C*). The influence of Δ^u on the mechanical restitution curve is demonstrated in Fig. 3 *D*.

Period of Quiescence. The most complex effect on mechanical restitution in trabeculae was obtained by interposing a stimulus pause before the test interval (see the protocol in the inset of Fig. 3 *E*). This intervention caused an increase of force at short test intervals (post-rest-potentiation), and a reduction at long test intervals. The model response is similar (Fig. 3 *E*). The reduced force at long intervals is due to the loss of Ca^{2+} from the exchange compartment during the 60-s pause. Since the pause-beat (p in the inset of Fig. 3 *E*) itself is of large amplitude, the recirculation fraction causes potentiation at the subsequent short interval. In the absence of recirculation ($r = 0$) there is no potentiation at the short test intervals (Fig. 3 *F*).

The responses of the model shown in Fig. 3 are very similar to the responses of ventricular trabeculae of rat heart (Schouten et al., manuscript submitted for publication). The three different types of mechanical restitution curves (Fig. 3, *A*, *C*, and *E*) demonstrate the different nature of postextrasystolic potentiation, frequency potentiation, and post-rest-potentiation.

Decay of Postextrasystolic Potentiation

In the trabeculae the decay of potentiation follows an exponential course (Fig. 4 *A*). It obeys the empirical recurrence relation

$$F(n+1) = D \cdot F(n) + \text{constant}, \quad (19)$$

where $F(n)$ is peak force of the nth beat of the negative staircase, and D is the empirical decay constant. D has been interpreted to represent the recirculation fraction r (Morad and Goldman, 1973; Wohlfart, 1979). The present model predicts that D is determined not only by r, but also by the three rate constants of Ca^{2+} transport: α, β, and γ. Simulations of the decay of postextrasystolic potentiation were performed for varying test frequencies (*inset*, Fig. 5 *A*) and for varying priming frequencies (*inset*, Fig. 6), using the parameter values given above.

TABLE I
VALUES OF THE MODEL PARAMETERS AS USED FOR THE SIMULATIONS SHOWN IN THE FIGURES

$\alpha = 1\ s^{-1}$	$\beta = 0.011\ s^{-1}$	$\gamma = 0.006\ s^{-1}$
$\Delta^u = 0.1$	$\Delta^e = 0.018$	$r = 0.65$

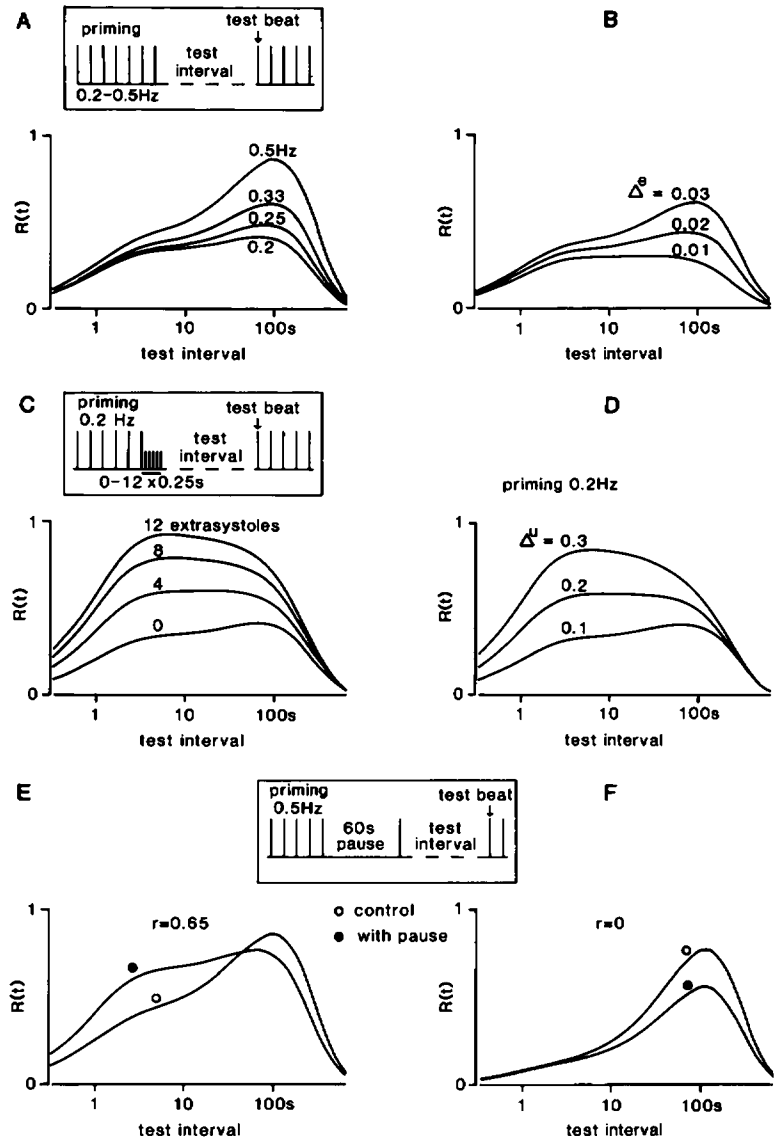

FIGURE 3 The influence of different stimulation protocols and of variation of model parameters on the simulated mechanical restitution curve. Variation of priming frequency (*A*) has a similar influence on the restitution curve as variation of Δ^e (*B*). The influence of extrasystoles (*C*) compares to the influence of Δ^u (*D*). Finally the increase of *F* at short intervals after a 50-s pause (*E*) is abolished when $r - 0$ (*F*). *Insets*: stimulation protocols.

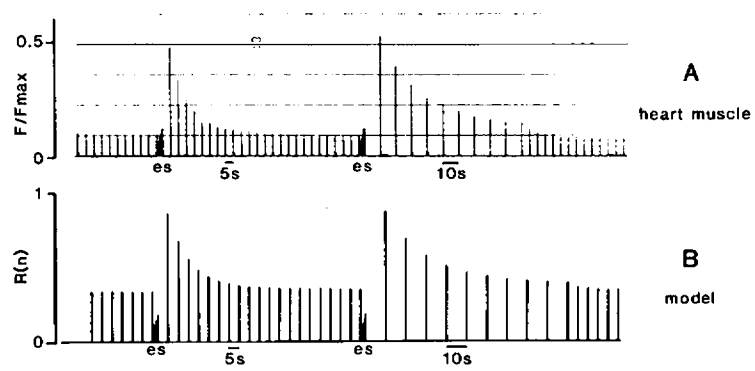

FIGURE 4 The exponential decay of postextrasystolic potentiation measured on a ventricular trabecula from rat heart (*A*) and simulated with the model (*B*). In the figure *es* stands for extrasystoles at 0.25-s intervals. F_{max} is the maximal force in the trabecula obtained in 2.5 mM Ca^{2+}. The recording was made in 0.8 mM Ca^{2+}, at 26°C.

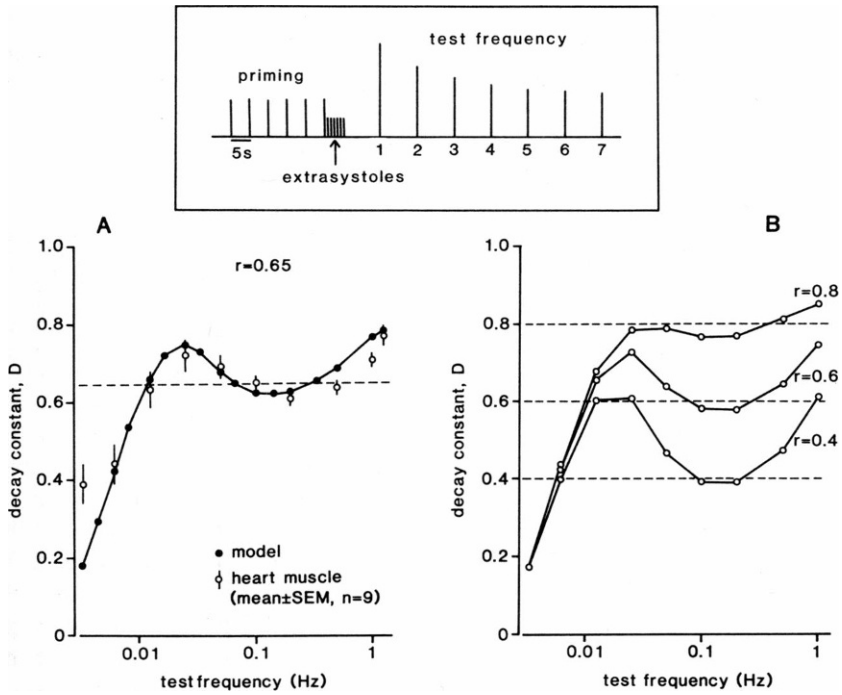

FIGURE 5 The influence of test frequency on the decay of post extrasystolic potentiation. The *inset* shows the stimulation protocol. The decay constant D was calculated according to Eq. 19 from test beats 1–8 (*inset*) for different test frequencies. In *A* the results of model simulations (*solid dots*) are compared with experimental data (*circles*). In *B* the influence of variation of r on the relationship between D and test frequency is shown.

Variation of Test Frequency. Fig. 4 *B* shows an example of the response of the model to extrasystoles and the negative staircase at different test frequencies. The plots of $F(n + 1)$ against $F(n)$ of the model simulations are linear, and D was calculated according to Eq. 19. D as a function of test frequency results in a curve very similar to that of heart muscle (Fig. 5 *A*). The dashed line in Fig. 5 *A* represents the value of r. It is obvious that D is a reasonable estimate of r at the limited frequency range from 0.3 to 0.03 Hz. This is exemplified in Fig. 5 *B*, which shows the influence of variation of r on D.

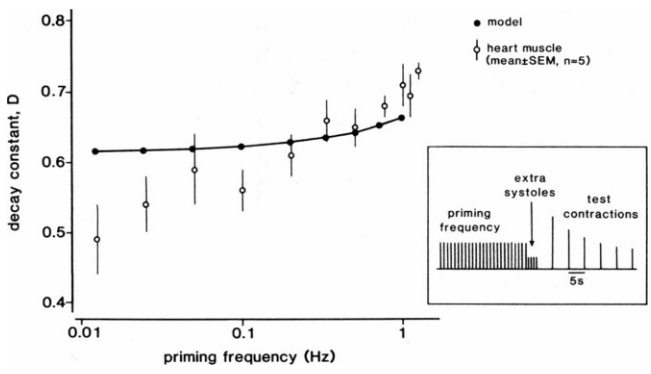

FIGURE 6 The influence of priming frequency on the decay of post extrasystolic potentiation. The stimulation protocol is depicted in the *inset*. The decay constant D was calculated according to Eq. 19 from test beats 1 to 8 (*inset*) for different priming frequencies. The results of model simulations (*solid dots*) and of experiments with a trabecula from rat heart (*circles*) are shown.

Variation of Priming Frequency. Variation of the priming frequency caused only a minor variation in D in the model responses. This contrasts the much larger variation in D in experiments with heart muscle (Fig. 6). Since in these experiments and simulations the test frequency was 0.2 Hz, the calculated D was probably representative for r, as argued above. Because in the model r is independent of the frequency, it follows that D is also independent of the frequency. It must be concluded that in the heart muscle, r increases with frequency and thereby D (Schouten et al., manuscript submitted for publication).

Effects of Nifedipine

Ca^{2+} influx during the action potential can be blocked in heart muscle by adding nifedipine to the superfusion medium (Mitchell et al., 1983). The effect of nifedipine on the mechanical restitution curve of a trabecula is shown in Fig. 7 *A*. Peak force was reduced predominantly at short test intervals. A similar effect on the simulated curve is obtained when $\Delta^u = 0$ (Fig. 7 *B*). In the presence of nifedipine the influence of a preceding 60-s pause on the mechanical restitution curve is very pronounced (Fig. 7 *C*). This effect is reproduced by the model when Δ^u is zero (Fig. 7 *D*).

Differences between Preparations

A large variation in the normalized steady state peak force (F_s/F_{max}) between preparations under the same experimental conditions has been reported, and a variation in the

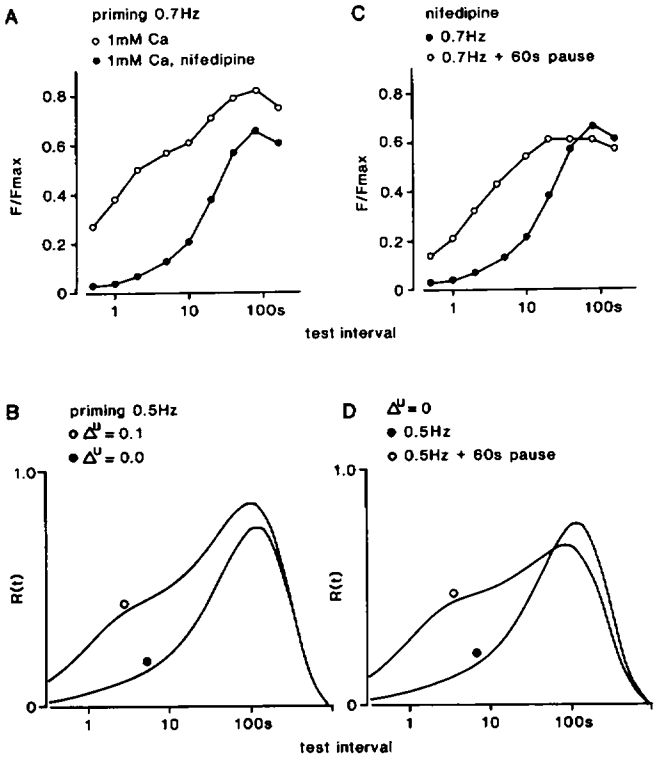

FIGURE 7 The influence of nifedipine on the mechanical restitution curve of a trabecula and of Δ^u on the simulated curve. (*A*) Restitution curves of a trabecula in 0.8 mM Ca^{2+} at a priming frequency of 0.7 Hz, in the absence (*circles*) and in the presence of nifedipine (0.1 mg/l). (*B*) The simulated restitution curves at a priming frequency of 0.5 Hz for $\Delta^u = 0.1$ (*circle*) and $\Delta^u = 0$ (*dot*). (*C*) Restitution curve of a trabecula in the presence of nifedipine at a priming frequency of 0.7 Hz (*solid dots*) and at the same priming frequency, but every test interval preceded by a 60-s pause (*circles*). (*D*) The simulated restitution curves for the same stimulation protocols as in *C*, for $\Delta^u = 0$.

decay constant D, and in the degree of potentiation obtained after one extrasystole ($\Delta F/F_{max}$) (Schouten et al., manuscript submitted for publication). The latter variable is the equivalent of the model parameter Δ^u. We have analyzed the correlations between the variables for the simple situation of stimulus intervals of 5 s. At these intervals D is approximately equal to r (Fig. 5 *A*) and the contribution of the exchange compartment to $R_T(n)$ can be neglected. Eq. 18 then (for $n = \infty$) reduces approximately to Eq. 20a, and the corresponding equation for the experimental variables is given by Eq. 20b

$$R_S(\infty) = \Delta^u/(1 - r) \quad (20a)$$

$$F_s/F_{max} = (\Delta F/F_{max})/(1 - D). \quad (20b)$$

The error in $R_S(\infty)$ introduced by the above approximation is ±16% for the data to be described below, using the values of α, β, γ, and Δ^e from Table I. From the preparations ΔF was measured as indicated in the inset of Fig. 8. F_s, ΔF, and D were measured from 39 preparations in one or more (maximum 5) Ca^{2+} concentrations, resulting in a total of 69 values of each variable (circles and dots in Fig. 8, *A–D*). The dots represent the values of 23 preparations in 0.8 mM Ca^{2+}, and these data were used for the following analysis. The model predicts no correlation between $\Delta F/F_{max}$ and $1/(1 - D)$, and thus the absence of a correlation in Fig. 8 *A* is in accordance with the model. A positive correlation is expected between F_s/F_{max} and $\Delta F/F_{max}$ and $1/(1 - D)$, and Fig. 8, *B* and *C* shows that this applies to the variations between the preparations. As expected from Eq. 20b, the highest correlation coefficient was found between F_s/F_{max} and $(\Delta F/F_{max})/(1 - D)$ as shown in Fig. 8 *D*. The slope of this relationship, however, was 0.44 (Fig. 8 *D*) instead of 1.0. A part of this deviation can be explained from the interval dependence of the action potential duration at 50% of its amplitude (APD_{50}). In a previous study (Schouten et al., manuscript submitted for publication) it has been shown that the magnitude of $\Delta F/F_{max}$ was closely linked to APD_{50}. The APD_{50} of the extrasystole (which determines ΔF) was prolonged by 50% as compared to the steady state APD_{50} (which contributes to F_s), i.e., it is probable that during the extrasystole ~50% more Ca^{2+} flows into the cell than during a steady state beat. The corresponding correction factor of 0.67 for ΔF in Eq. 20b would result in a slope of 0.66. The cause of the remaining deviation of the slope is unknown.

The analysis above applies to the 23 preparations in 0.8 mM Ca^{2+}, and the results indicate that Eq. 20b is useful for the analysis of the variations between preparations under the same conditions. The analysis equally applies to the variations between preparations in different Ca^{2+} concentrations (the correlation coefficients are given in the legend of Fig. 8).

Post-Rest Depression of Peak Force

If stimulation is resumed after a 100-s pause, then the first beat is potentiated because it is at the maximum of the restitution curve. Due to the recirculating fraction, the next beats are also potentiated, but progressively less. Generally, this descending staircase creates an undershoot of peak force, and is followed by an ascending staircase to the steady state peak force at the given frequency of stimulation. The polyphasic transient after a pause has been observed in atrial and ventricular heart muscle of mammals (Koch-Weser and Blinks, 1963). For Fig. 9 the results from two ventricular trabeculae from rat heart were selected that showed large quantitative differences. The preparation of Fig. 9 *A* showed a small effect of an interpolated extrasystole ($\Delta F = 0.037 \cdot F_{max}$, *left*), which may indicate a small influx of Ca^{2+} during the action potential (Δ^u).

The decay of potentiation was relatively slow (D = 0.77), indicating a large recirculating fraction (r), and post-rest potentiation was strong (*right*). Postextrasystolic potentiation was strong in the preparation used for Fig. 9 *C* ($\Delta F = 0.32$). The decay of potentiation was rapid (D = 0.51) and post-rest potentiation was weak in this preparation. Peak force declined to below the steady state level

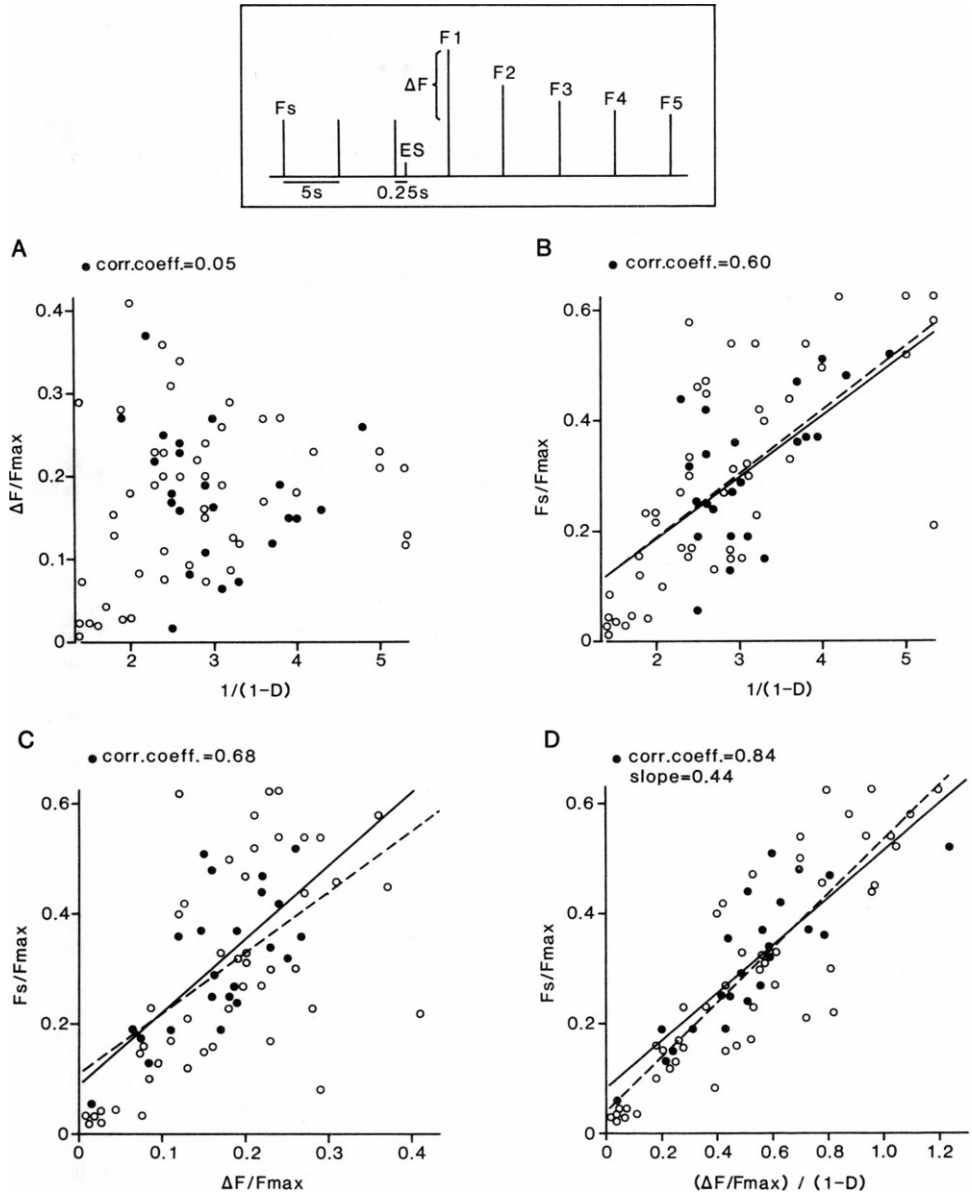

FIGURE 8 Analysis of the variations in F_s/F_{max}, $\Delta F/F_{max}$ and in D between different preparations in different Ca^{2+} concentrations. The *inset* shows a schematical representation of the stimulation protocol and the variations in peak force (*ES* = extrasystole). In all graphs the data points reflect the values of the variables as obtained from 39 preparations in 0.2–1.0 mM Ca^{2+} (one to five different concentrations per preparation). The data from 23 preparations in 0.8 mM Ca^{2+} are indicated by the solid dots. The correlation coefficients given above each graph were calculated from the data in 0.8 mM Ca^{2+} only. The lines represent the least-squares linear fit for the dots (*solid lines*) and for all data (*dashed lines*). The correlation coefficients for all data per graph were (*A*) 0.09, (*B*) 0.70, (*C*) 0.57, and (*D*) 0.87. The correlation coefficients given above each graph apply to the 23 data in 0.8 mM Ca^{2+} only. The intervals of 95% confidence of these coefficients, calculated according to the jackknife method (Parr, 1983) were (*B*) 0.24–0.96, (*C*) 0.34–1.0, (*D*) 0.60–1.0. The differences between the correlation coefficients in *D* and *B* ($p = 0.06$) and in *D* and *C* ($p = 0.15$) were not significant.

(indicated by dashed lines) in both preparations and the undershoot is more pronounced after longer pauses. The model reproduced the undershoot and after adjustment of the parameter values, it also reproduced the quantitative differences, as shown in Fig. 9, *B* and *E*. The phenomena of post-rest potentiation and of post-rest depression (undershoot) reflect the kinetics of the exchange compartment. From Fig. 6 it was concluded that the recirculating fraction (or its physiological equivalent) in heart muscle decreases at low frequencies, or after a long pause. In the model, r is a constant, and this may explain the fact that for a reasonable simulation, the parameters r and Δ^u had to be taken much smaller in Fig. 9 *D*, than the physiological variables D and ΔF in Fig. 9 *C*. In the Discussion it is argued that the recirculating fraction and the content of the hypothetical exchange compartment are probably related to the intracellular Na^+-concentration, the kinetics of the Na^+/K^+ pump, and the Na^+/Ca^{2+} exchange mech-

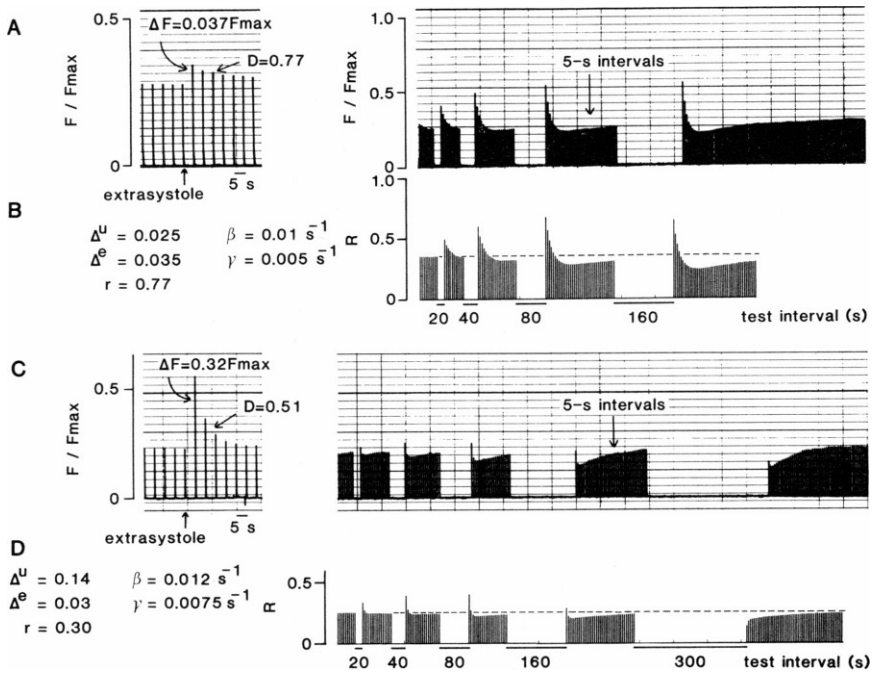

FIGURE 9 Post-rest depression of peak force in heart muscle and in the model simulations. Two preparations were selected that showed large quantitative differences, in the degree of postextrasystolic potentiation and in the decay constant D (*left* in *A* and *C*). The indicated values of D were calculated from the decay of potentiation after 4 and 10 extrasystoles in both preparations. The model parameters were adjusted in *B* to obtain a simulation of the muscle response in *A*, and in *D* to simulate the response in *C*. The dashed lines indicate the steady state peak force, and were drawn to accentuate the post-rest depression of peak force.

anism. This explains the positive correlation between D and the amplitude of the late maximum in the restitution curve as obtained by variation of $[Ca^{2+}]_o$ and priming frequency in heart muscle (Schouten et al., manuscript submitted for publication). The positive correlation between D and the amplitude of the late maximum in Fig. 9, *A* and *C* is in accordance with this idea.

DISCUSSION

The present model (Fig. 1 *B*) is an extension of the conventional two-compartment model (see Introduction). The new feature is an exchange compartment, which was postulated to account for the slow phases of mechanical restitution in isolated heart muscle of the rat (Fig. 1 *A*). Through experiments it was evidenced that peak force at the short and long test intervals can be varied independently (Schouten et al., manuscript submitted for publication). This property is represented by the terms $f \cdot U_o$ and $g \cdot E'_o$ in Eq. 18. A few assumptions were made to simplify the model to the minimum number of six independent parameters. The resulting analytical solution (Eq. 18) allows for fast computer simulations. The mathematical model reproduced the various force-interval relationships observed in heart muscle (Figs. 3–5, and 7), and offers an explanation for the different nature of three types of potentiation. (*a*) Postextrasystolic potentiation is due to Ca^{2+} accumulation in the uptake compartment and therefore causes an increase of the early component of restitution (Fig. 3 *A*). (*b*) Frequency potentiation is primarily due to Ca^{2+} accumulation in the exchange compartment and causes an increase of the late component predominantly (Fig. 3 *C*). (*c*) Post-rest potentiation: After a 60-s pause peak force is near the maximum of restitution. The associated large amount of released Ca^{2+} partly recirculates via the uptake compartment. During the 60-s pause, however, Ca^{2+} is gradually lost from the exchange compartment. Therefore the restitution curve determined after a pause shows an increase of the early component, but a decrease of the late component (Fig. 3 *E*).

The experiments with nifedipine demonstrate the value of the model for analysis of the effects of drugs. Nifedipine blocks the Ca^{2+} influx during excitation (Henry, 1980; Church and Zsoter, 1980). Probably it does not inhibit the Na^+/Ca^{2+} exchange mechanism (Schouten and ter Keurs, 1985), which may be involved in the exchange compartment (Schouten et al., manuscript submitted for publication). The selective reduction of the early phase of restitution (Fig. 7 *A*) is in agreement with this idea and the effect can be simulated by the model when $\Delta^u = 0$ (Fig. 7 *C*). Also in agreement are the facts that nifedipine abolishes postextrasystolic potentiation but does not affect frequency potentiation (not shown) and post-rest potentiation (Fig. 7, *B* and *D*).

This model was based on the analysis of mechanical restitution in rat ventricular muscle. It should be noted, however, that a late maximum in the restitution curve has

been obtained at 30 s from cat papillary muscles (Allen et al., 1976) and at 100 s from human ventricular trabeculae (Quaegebeur et al., 1986) when either $[Ca^{2+}]_o$ or the priming frequency was high. Probably the model applies to heart muscle in general, but the best fitting values of the parameters vary between species.

Interpretation of the Compartments

The uptake and release compartments are probably located in the sarcoplasmic reticulum of the muscle fibers. An ATPase with high affinity to Ca^{2+} has been identified in the longitudinal tubuli. Through this pump, the reticulum accumulates Ca^{2+}. Excitation-dependent release of Ca^{2+} may occur at the terminal cisternae that are associated with the sarcolemma (for reviews, see Katz, 1976; Blayney, 1983; Carafoli, 1985). It is less clear which structure or mechanism is represented by the exchange compartment. The function of this compartment in the model was to enable the derivation of a simple function, which describes the two slow phases of mechanical restitution, i.e., the ascending limb (β in Fig. 1 *A*) to the maximum at 100 s, and the descending limb (γ in Fig. 1 *A*). In previous studies, these two phases have always been analyzed separately. Generally, force declines at intervals longer than a few seconds in heart muscle of species other than the rat, at moderate $[Ca^{2+}]_o$, and the late maximum is absent. The descending limb has been attributed to leakage from the sarcoplasmic reticulum in series with a small efflux from the cells via Na^+/Ca^{2+} exchange (Bass, 1976; Allen et al., 1976). To explain the increase of force to the maximum at 100 s, Ragnarsdottir et al. (1982) postulated that in rat heart there would be a small influx during rest, until the Ca^{2+} content of the cells is in equilibrium with the extracellular Ca^{2+}. Thereby, however, they ignored the descending limb of the restitution curve in rat heart.

Nevertheless, the above explanations of the ascending and descending limbs of the restitution curve (β and γ in Fig. 1 *A*) can be combined, and we propose that the late maximum reflects a small net influx on Ca^{2+} that decays with time to become a net outward flux after ~100 s. The explanation may be as follows: It is generally accepted that frequent stimulation leads to intracellular accumulation of Na^+ (Cohen and Fozzard, 1982; Lee and Dagostino, 1982). This would reduce the efflux and enhance the influx of Ca^{2+} via Na^+/Ca^{2+} exchange (Reuter, 1974; Mullins, 1979; Johnson and Kootsey, 1985), i.e., a rise of $[Na^+]_i$ results in a rise of $[Ca^{2+}]_i$ and an increase of peak force (Daut, 1982; Sheu and Fozzard, 1982; Chapman et al., 1983). During rest, $[Na^+]_i$ declines with a time constant of 20–100 s, due to the activity of the Na^+/K^+ pump (Gadsby and Cranefield, 1979; Lee and Dagostino, 1982; Eisner et al., 1984) and, as a consequence, the net influx of Ca^{2+} will become less and eventually become a net efflux. Crucial to this hypothesis is the assumption that the sarcoplasmic reticulum continues to accumulate Ca^{2+} during rest, until the sarcoplasmic concentration of free Ca^{2+} has dropped to a very low level and Ca^{2+} uptake becomes less than the leakage from the reticulum. The hypothesis is attractive as it relies mainly on well-known mechanisms. According to our interpretation, the exchange compartment was postulated to obtain a simple and abstract description of the slow phases of mechanical restitution (see Definition of the Minimum Model), whereas the Na^+/Ca^{2+} exchanger and the Na^+/K^+ pump may be the underlying fundamental mechanisms.

Decay of Potentiation

Postextrasystolic potentiation and the subsequent exponential decay have been described many times in literature for isolated heart muscle (e.g., Hoffman et al., 1956; Scriabine, 1959; Garb and Penna, 1956) and also for the heart in situ (Elzinga et al., 1980; Yellin et al., 1979). The response of the model to extrasystoles is similar (Fig. 4). The potentiation is due to Ca^{2+} accumulation in the uptake compartment. The decay followed an exponential course and obeyed the empirical recurrence relation (Eq. 19). The decay constant D (see Eq. 19) varied with the test frequency in a complex way. Between 0.3 and 0.1 Hz, D was almost equal to r (Fig. 5 *B*). At higher frequencies, however, the rate constant α causes an increase of D. At lower frequencies D is predominantly determined by the rate constants β and γ. It has been reported that D is fairly constant over the frequency range of 1–0.01 Hz, and this has been regarded as evidence for a constant recirculation fraction (Morad and Goldmann, 1973). The present analysis shows that the relatively small variation of D at this frequency range reflects a mere coincidence of the combined influence of four independent parameters. This result illustrates the value of the present model.

Influence of Priming Frequency

In the model simulation the decay constant in almost independent of the priming frequency, in contrast to the much stronger dependence observed in heart muscle (Fig. 6). At the test frequency used (0.2 Hz), D is predominantly determined by r as discussed above. Therefore, it has been concluded that the physiological equivalent of r in the muscles is probably frequency dependent (Schouten et al., manuscript submitted for publication). This can be explained as follows. Extrusion of Ca^{2+} during the contractions probably occurs via the Na^+/Ca^{2+} exchange mechanism (Hoerter and Vassort, 1982; Schouten and ter Keurs, 1985). With increasing stimulation frequency, Na^+ accumulates in the cells (Cohen et al., 1982) and this inhibits Ca^{2+} extrusion via $Na+/Ca^{2+}$ exchange. Hence, the extruded fraction, $1 - r$, will decrease, i.e., the recirculation fraction, r, will increase. To incorporate such an effect in the model, r may be related to the content of the exchange compartment.

Variations between Preparations

The F_s/F_{max} varied by a factor of 10 between preparations under the same experimental condition (0.2 Hz, 0.8 mM Ca^{2+}; Fig. 8, solid dots). The analysis shown in Fig. 8, *A–D* has interesting implications: (*a*) It has been shown that F_s, ΔF, and D increase with the extracellular Ca^{2+} concentration (Schouten et al., manuscript submitted for publication). It follows that for each individual preparation a positive correlation can be found among the three variables. In the presence of nifedipine, however, ΔF (Δ^u in the model) was reduced (Fig. 7, *A* and *B*), whereas the recirculation of Ca^{2+}, and thereby D, was unaffected (Fig. 7, *C* and *D*). Further evidence for independent variation in ΔF and D is given in Fig. 8 *A*. An important conclusion is that ΔF and D are two independent determinants of the force of contraction that can be measured in the intact preparations. (*b*) Previous attempts to analyze transient phenomena of contractility of the heart by means of D and action potential duration have been successful for the rabbit heart in situ. A positive correlation was found between peak force of a given beat and both the peak force and the action potential duration of the preceding beat (Wohlfart and Elzinga, 1982). The same analysis did not apply, however, to the intact dog heart (Elzinga et al., 1981). These results indicate that the variable ΔF can be used instead of the action potential duration. (*c*) The heart in situ is subject to the influence of mechanisms that regulate blood pressure through the contractility of the heart. This may mean that if ΔF, for instance, is affected by some pathological condition, a compensatory change of D may occur. The result would be a negative correlation between the values of ΔF and D obtained from different individuals. It follows that the present results probably will not apply to the heart in situ in every detail. Eq. 20b, however, may serve to analyze not only transient phenomena, but also the steady state contractility, and to characterize diseased heart muscle.

Shortcomings of the Model

Although the model presented in this paper offers an explanation for a variety of phenomena, the following limitations must be noted: (*a*) As mentioned in the mathematical section, peak force is assumed to be proportional to the amount of released Ca^{2+}. In myocardial preparations maximal peak force is obviously limited by saturation of one of the Ca^{2+} handling mechanisms (Schouten et al., manuscript submitted for publication). Saturation kinetics are not incorporated in the present model.

(*b*) The processes of contraction and excitation are assumed to last an infinitesimally short time. Therefore, the model probably does not apply to phenomena occurring at intervals shorter than ~0.5 s, i.e., close to the duration of a contraction.

(*c*) As argued above, the recirculating fraction is probably influenced by stimulation frequency and not a constant, as in the present model.

(*d*) Ca^{2+} influx during the action potential is reduced when the intracellular Ca^{2+} concentration is high, i.e., during strong contractions (Mitchell et al., 1983; Josephson et al., 1984). This phenomenon has been interpreted as a negative feedback mechanism that tends to prevent excessive Ca^{2+} loading of the cells (Braveny and Sumbera, 1970; Bassingthwaighte et al., 1976). The observed prolongation of the action potential during a weak extrasystole is in accordance with this hypothesis (Schouten, 1984; Schouten et al., manuscript submitted for publication), and the phenomenon was used to explain the deviating slope in Fig. 8 *D*. Although good simulations of mechanical restitution and of decay of potentiation were produced by the model, the analysis given in Fig. 8 indicates that the model should be extended with a parameter for the negative feedback mechanism.

(*e*) As shown by Hilgeman et al. (1983), a transient accumulation or depletion of Ca^{2+} may occur in the interstitium upon a change of stimulation frequency. This may affect the time course of the positive and negative force staircases. To meet such effects the model should be extended with a limited interstitial space.

(*f*) In the early version of the two-compartment model it has been postulated that the release compartment releases only a fraction of its Ca^{2+} content upon excitation (Antoni et al., 1969; Braveny and Sumbera, 1970; Manring and Hollander, 1971). In later versions of the model this fractional-release-hypothesis has been replaced by the "recirculating-fraction-hypothesis" (Morad and Goldman, 1973; Edman and Johannsson, 1976). Recently Fabiato (1984) reported evidence in support of the fractional-release-hypothesis, however, he also assumed intracellular recirculation of Ca^{2+}. The present results do not justify to extend the model with a parameter for fractional release.

(*g*) After a very long period of quiescence, the first contraction will be independent of the proceeding stimulation pattern. This so-called "rested state contraction" is generally weak in ventricular, but strong in atrial muscle of mammals (Koch-Weser and Blinks, 1963). In rat ventricular muscle, the rested state contraction can be measured after ~20 min of quiescence. At 1 mM Ca^{2+}, it shows a large variation and ranges from 0.1 to 0.7 F_{max} (unpublished observations). From Eq. 10 it is clear that $R(\infty)$ approaches zero, and that the model does not reproduce rested state contractions. To incorporate this property, a constant small influx, j_e, into the exchange compartment may be postulated. Thus, by substituting $j'_e = j_e \cdot V_r/V_e$ (see Eq. 6) it follows that

$$R(\infty) = E'(\infty) = j'_e/\gamma \quad (21)$$

$$R(t) = f \cdot U_o + g \cdot E'_o + (1 - g - e^{-\beta t}) \cdot j'_e/\gamma. \quad (22)$$

In conclusion, the model developed responds to many different stimulation patterns in a similar way as isolated heart muscle. The model may be a valuable tool for the analysis of the site of action of drugs, as was indicated by

the simulations of the effects of nifedipine. Since it was possible to analyze the differences between preparations by means of the model, it may serve to evaluate pathological conditions in the intact heart.

We wish to thank Mrs. Iris de Goede and Mrs. Jacqueline van Dam for typing the manuscript, and Mr. Hans Kleijn for technical assistance.

This work was supported by the Foundation for Medical Research FUNGO (grant No. 13-22-75).

Received for publication 25 June 1985 and in final form 23 July 1986.

REFERENCES

Adler, D., A. Y. K. Wong, Y. Mahler, and G. A. Klassen. 1985. Model of calcium movements in the mammalian myocardium: interval-strength relationship. *J. Theor. Biol.* 113:379–394.

Allen, D. G., B. R. Jewell, and E. H. Wood. 1976. Studies of the contractility of mammalian myocardium at low rates of stimulation. *J. Physiol. (Lond.).* 254:1–17.

Antoni, H., R. Jacob, and R. Kaufmann. 1969. Mechanische Reaktionen des Frosch- und Säugetiermyokards bei Veränderung der Aktionspotential-Dauer durch konstante Gleichstromimpulse. *Pfluegers Arch.* 306:33–57.

Bass, O. 1976. The decay of the potentiated state in sheep and calf ventricular myocardial fibers. *Circ. Res.* 39:396–399.

Bassingthwaighte, J. B., C. H. Fry, and J. A. S. McGuigan. 1976. Relationship between internal calcium and outward current in mammalian ventricular muscle; a mechanism for the control of action potential duration? *J. Physiol. (Lond.).* 262:15–37.

Blayney, L. 1983. Cardiac sarcoplasmic reticulum. *In* Cardiac Metabolism. A. J. Drake-Holland and M. I. M. Noble, editors. John Wiley & Sons, Chichester.

Blinks, J. R., and J. Koch-Weser. 1961. Analysis of the effects of changes in rate and rhythm upon myocardial contractility. *J. Pharmacol. Exp. Ther.* 133:373–389.

Braveny, P., and J. Sumbera. 1970. Electromechanical correlations in the mammalian heart muscle. *Pfluegers Arch.* 319:36–48.

Carafoli, E. 1985. The homeostasis of calcium in heart cells. *J. Mol. Cell. Cardiol.* 17:203–212.

Chapman, R. A., A. Coray, and J. A. S. McGuigan. 1983*a*. Sodium/calcium exchange in mammalian ventricular muscle: a study with sodium-sensitive micro-electrodes. *J. Physiol. (Lond.).* 343:253–276.

Church, J., and T. T. Zsoter. 1980. Calcium antagonistic drugs. Mechanism of action. *Can. J. Physiol.* 58:254–246.

Cohen, C. J., H. A. Fozzard, and S.-S. Sheu. 1982. Increase of intracellular sodium ion activity during stimulation in mammalian cardiac muscle. *Circ. Res.* 50:651–662.

Daut, J. 1982. The role of intracellular sodium ions in the regulation of cardiac contractility. *J. Mol. Cell. Cardiol.* 14:189–192.

DiStefano J. J., and E. M. Landaw. 1984. Multiexponential, multicompartmental, and noncompartmental modeling. I. Methodological limitations and physiological interpretations. *Am. J. Physiol.* 246:R651–R664.

Edman, K. A. P., and M. Johannsson. 1976. The contractile state of rabbit papillary muscle in relation to stimulation frequency. *J. Physiol (Lond.).* 254:565–581.

Eisner, D. A., W. J. Lederer, and R. D. Vaughan-Jones. 1984. The electrogenic Na pump in mammalian cardiac muscle. *In* Electrogenic Transport: Fundamental Principles and Physiological Implication. M. P. Blaustein and M. Lieberman, editors. Raven Press, New York.

Elzinga, G., M. J. Lab, M. I. M. Noble, D. E. Papadoyannis, J. Pidgeon, A. Seed, and B. Wohlfart. 1981. The action potential duration and contractile response of intact heart related to the preceding interval and the preceding beat in the dog and cat. *J. Physiol. (Lond.).* 314:481–500.

Fabiato, A. 1983. Calcium-induced release of calcium form the cardiac sarcoplasmic reticulum. *Am. J. Physiol.* 245:C1–C14.

Fabiato, A. 1984. Ca^{2+}-induced release of Ca^{2+} from the sarcoplasmic reticulum of skinned canine cardiac Purkinje cells. *Proc. Physiol. Soc.* March. S6.

Fozzard, H. A. 1977. Heart: Excitation-contraction coupling. *Annu. Rev. Physiol.* 39:210–220.

Gadsby, D. C., and P. F. Cranefield. 1979. Electrogenic sodium extrusion in cardiac Purkinje fibers. *J. Gen. Physiol.* 73:819–837.

Garb, S., and M. Penna. 1956. Some quantitative aspects of the relation of rhythm to the contractile fore of mammalian ventricular muscle. *Am. J. Physiol.* 184:601–606.

Garfinkel, D., and K. A. Fegley. 1984. Fitting physiological models to date. *Am. J. Physiol.* 246:R641–R650.

Henry, P. D. 1980. Comparative pharmacology of calcium antagonists: nifedipine, verapamil and diltiazem. *Am. J. Cardiol.* 46:1047–1058.

Hilgemann, D. W., M. J. Delay, and G. A. Langer. 1983. Activation-dependent cumulative depletions of extracellular free calcium in guinea pig atrium measured with antipyrylazo III and tetramethylmurexide. *Circ. Res.* 53:770–793.

Hoerter, J. A., and G. Vassort. 1982. Participation of the sarcolemma in the control of relaxation of the mammalian heart during perinatal development. *In* Advances in Myocardiology. 3. C. Charov, V. Smirnov, and N. S. Dhalla, editors. Plenum Publishing Corp., New York.

Hoffman, B. F., E. Bindler, and E. E. Suckling. 1956. Postextrasystolic potentiation of contraction in cardiac muscle. *Am. J. Physiol.* 185:95–102.

Johnson, E. A., and J. M. Kootsey. 1985. A minimum mechanism for Na-Ca exchange: net and unidirectional Ca fluxes as function of ion composition and membrane potential. *J. Membr. Biol.* 86:167–187.

Josephson, I. R., J. Sanchez-Chapula, and A. M. Brown. 1984. A comparison of calcium current in rat and guinea pig single ventricular cells. *Circ. Res.* 54:144–156.

Katz, A. M. 1976. Tonic and phasic mechanisms in the regulation of myocardial contractility. *Basic Res. Cardiol.* 71:447–455.

Kaufmann, R., R. Bauer, T. Fürniss, H. Krause, and H. Tritthart. 1974. Calcium movement controlling cardiac contractility. II. Analog computation of cardiac excitation-contraction coupling on the basis of calcium kinetics in a multicompartment model. *J. Mol. Cardiol.* 6:543–559.

Koch-Weser, J., and J. R. Blinks. 1963. The influence of the interval between beats on myocardial contractility. *Pharmacol. Rev.* 15:601–652.

Landau, M., and F. A. Valentini. 1982. Construction, mathematical study and numerical simulation of a calcium turnover model during skeletal muscle contraction. *Int. J. Bio-Med. Comp.* 13:49–68.

Lee, C. O., and M. Dagostino. 1982. Effect of strophantidin on intracellular Na ion activity and twitch tension of constantly driven canine Purkinje fibers. *Biophys. J.* 40:185–198.

Manring, A., and P. B. Hollander. 1971. The interval — strength relationship in mammalian atrium: a calcium exchange model. *Biophys. J.* 11:483–501.

Markhasin, V. S., and G. N. Mil'shtein. 1979. Modelling the influence of rhythm on the force of contraction of heart muscle. *Biophysics.* 23:688–696.

Mitchell, M. R., T. Powell, D. A. Terrar, and V. W. Twist. 1983. Characteristics of the second inward current in cells isolated from rat ventricular muscle. *Proc. R. Soc. Lond. B Biol. Sci.* 219:447–469.

Morad, M., and Y. Goldman. 1973. Excitation-contraction coupling in heart muscle: membrane control of development of tension. *Prog. Biophys. Mol. Biol.* 27:257–313.

Mullins, L. J. 1977. A mechanism for Na/Ca transport. *J. Gen Physiol.* 70:681–695.

Mullins, L. J. 1979. The generation of electric current in cardiac fibers by Na/Ca exchange. *Am. J. Physiol.* 263:C103–C110.

Parr, W. C. 1983. A note on the jackknife, the bootstrap and the delta method estimators of bias and variance. *Biometrika.* 70:719–722.

Posner, C. J., and D. A. Berman. 1967. A mathematical analysis of the interval-strength relationship in the rat ventricular strip and its modification by fluoroacetate. *J. Pharmacol Exp. Ther.* 156:166–177.

Quaegebeur, J. M., V. J. A. Schouten, and H. E. D. J. ter Keurs. 1986. Mechanical restitution in isolated human heart muscle. *J. Physiol. (Lond.).* 377:120.

Ragnarsdottir, K., B. Wohlfart, and M. Johansson. 1982. Mechanical restitution in rat papillary muscle. *Acta Physiol. Scand.* 115:183–318.

Reuter, H. 1974. Exchange of calcium ions in the mammalian myocardium: mechanisms and physiological significance. *Circ. Res.* 34:599–605.

Schouten, V. J. A. 1984. The relationship between action potential duration and force of contraction in rat myocardium. *Eur. Heart J.* 5:984–992.

Schouten, V. J. A., and H. E. D. J. ter Keurs. 1985. The slow repolarization phase of the action potential in rat heart. *J. Physiol. (Lond.).* 360:13–25.

Scriabine, A. 1959. Uber die Anderung der Kontraktions-amplitude des elektrisch gereizten Rattenpapillarmuskels nach einer reizpause oder einer Periode hochfrequenter Reizung. *Pfluegers Arch.* 269:311–318.

Sheu, S-S., and H. A. Fozzard. 1982. Transmembrane Na^+ and Ca^{2+} electrochemical gradients in cardiac muscle and their relationship to force development. *J. Gen. Physiol.* 80:325–351.

Tsaturyan, A. K., and V. Ya. Izakow. 1979. Mathematical model of the coupling of excitation with contraction in the heart muscle. *Biophysics.* 23:904–910.

Wallinga-de Jonge, W., H. B. K. Boom, R. J. Heijink, and G. H. van der Vliet. 1981. Calcium model for mammalian skeletal muscle. *Med. Biol. Eng. Comput.* 19:734–748.

Wohlfart, B. 1979. Relationship between peak force, action potential duration and stimulus interval in rabbit myocardium. *Acta Physiol. Scand.* 106:395–409.

Wohlfart, B. 1982. Interval-strength relation of mammalian myocardium interpreted as altered kinetics of activator calcium during the cardiac cycle. University of Lund, Ph.D. Thesis.

Wohlfart, B., and G. Elzinga. 1982. Electrical and mechanical responses of the intact rabbit heart in relation to the excitation interval. *Acta Physiol. Scand.* 115:331–340.

Wohlfart, B., and M. I. M. Noble. 1982. The cardiac excitation-contraction cycle. *Pharm. Ther.* 16:1–43.

Wong, A. Y. 1981. A model of excitation-contraction coupling of mammalian cardiac muscle. *J. Theor. Biol.* 90:37–61.

Yellin, E. L., A. Kennish, C. Yoran, S. Laniodo, N. M. Buckley, and R. W. M. Frater. 1979. The influence of left ventricular filling on postextrasystolic potentiation in the dog heart. *Circ. Res.* 44:712–722.